Genes & Diseases (2019) 6, 398–406

Available online at www.sciencedirect.com

ScienceDirect

journal homepage: http://ees.elsevier.com/gendis/default.asp

FULL LENGTH ARTICLE

Role of rno-miR-124-3p in regulating MCT1 expression in rat brain after permanent focal cerebral ischemia

Shi-ye Xu, Xu-li Jiang, Qian Liu, Jin Xu, Juan Huang, Sheng-wei Gan, Wei-tian Lu, Fei Zhuo, Mei Yang, Shan-quan Sun*

Department of Anatomy, Chongqing Medical University 1 Yixueyuan Road, Yuzhong District, China

Received 29 October 2018; accepted 14 January 2019
Available online 16 February 2019

KEYWORDS
Cerebral ischemia;
Lactate acid;
Monocarboxylate transporters (MCTs);
microRNAs (miRNAs);
Permanent middle cerebral artery occlusion (pMCAO)

Abstract This study aimed to assess the role of microRNAs (miRNAs) in regulating monocarboxylate transporter-1 (MCT1) expression in rat brain after permanent focal cerebral ischemia to identify a new target for early treatment of cerebral ischemia. Focal cerebral ischemia was induced by permanent middle cerebral artery occlusion (pMCAO) in rats. Morphology and protein expression levels of MCT1 were assessed by immunofluorescence and Western blotting. Using bioinformatics and double luciferase reporter assays, rno-miR-124-3p was selected as a direct target for rat MCT1. Expression of rno-miR-124-3p after pMCAO was detected. Then, rats were treated with rno-miR-124-3p agomir via lateral ventricle injection, and after 6 h or 24 h ischemia, rno-miR-124-3p expression and gene and protein expression of MCT-1 were detected by qRT-PCR and Western blotting. Brain infarction was identified by 2, 3, 5-triphenyltetrazolium chloride (TTC) staining. Results showed that pMCAO induced brain infarction and increased the expression of MCT1. The levels of rno-miR-124-3p after pMCAO were in contrast to those of MCT1 protein in ischemic region, while declined after 3, 6 and 12 h of pMCAO in ischemic penumbra. After administration of rno-miR-124-3p agomir, MCT1 mRNA and protein levels were increased after 6 h of pMCAO, while decreased after 24 h of pMCAO. Meanwhile, rno-miR-124-3p levels increased after both times. TTC staining showed treatment with rno-miR-124-3p agomir reduced brain infarction. The role of rno-miR-124-3p in regulating MCT1 was as a positive regulator after 6 h of pMCAO, while a negative regulator after 24 h of pMCAO, however, both activities had protective effects against cerebral ischemia.

* Corresponding author.
E-mail address: sunsq2151@cqmu.edu.cn (S.-q. Sun).
Peer review under responsibility of Chongqing Medical University.

https://doi.org/10.1016/j.gendis.2019.01.002

Introduction

Stroke, including ischemic and hemorrhagic stroke, is one of the main causes of death and permanent disability worldwide, and ischemic stroke accounts for at least 85% of all stroke cases.[1,2] Glucose has long been considered the only substrate supporting brain energy needs. However, the astrocyte-neuron lactate shuttle (ANLS) hypothesis, proposed by Pellerin and Magistretti, marked a turning point in the understanding of neuroenergetics.[3] Since then, attention has been increasingly paid to other cerebral energy substrates, such as lactate and ketone bodies.[4,5] Currently, lactate is considered an important, if not the main, cerebral alternative substrate to glucose.[6–8] The vast majority of stroke cases are associated with severe cerebral lactic acidosis, which is a key factor leading to permanent brain cell damage.[9] Acute stressful events such as stroke can precipitate metabolic shifts, leading to increased lactate production and the modulation of monocarboxylate transporters (MCTs) that control lactate levels.[10,11] MCTs constitute a family of 14 transmembrane proteins encoded by the *Slc16a* family of genes.[12] In the brain, MCTs control the delivery of lactate produced by astrocytes to neurons, where it acts as oxidative fuel.[13] Moreover, MCT1 is the most prominent monocarboxylic acid transporter in the cerebral microvascular endothelium.[9] Thus, factors that regulate MCT1 function may be critical in controlling the extent of lactic acidosis and therefore brain damage during stroke. However, the expression and regulatory mechanisms of MCT1 in cerebral ischemia remain undefined. Thus, it is of great significance for the treatment of cerebral ischemia to understand the MCT1 expression changes during cerebral ischemia and its possible regulatory mechanisms.

MicroRNAs (miRNAs) are single-stranded, endogenously expressed noncoding RNA molecules of ~22 nucleotides in length.[14] They post-transcriptionally regulate gene expression by binding to the 3′-untranslated region (3′-UTR) of target mRNAs through base-pairing and subsequently disable them or inhibit their translation.[14,15] Multiple miRNAs have been reported to be brain enriched or even brain specific.[16] Increasing evidence indicates significant roles of miRNAs in the response to cerebral ischemia.[2,16] Indeed, many studies have demonstrated that more than 20% of miRNAs are altered in the ischemic brain, indicating that miRNAs might emerge as key mediators in both pathogenic and pathological aspects of ischemic stroke.[17–19] However, it is unclear whether miRNAs can regulate MCT1 and thus be involved in the treatment of cerebral ischemia.

Therefore, this study assessed the roles of miRNAs in MCT1 regulation during cerebral ischemia in rats after permanent middle cerebral artery occlusion (pMCAO). Our findings provide a new basis for the early treatment of cerebral ischemia.

Materials and methods

Animals

Healthy male Sprague-Dawley rats (200–220 g), obtained from the Animal Centre of Chongqing Medical University, were maintained with standard laboratory chow and drinking water ad libitum. The experiments began after three days of feeding adaptation. All animal experiments were performed in accordance with the approval of the Ethics Committee of Chongqing Medical University.

Model establishment

Permanent focal cerebral ischemia was induced by left middle cerebral artery occlusion using the permanent middle cerebral artery occlusion (pMCAO) method based on the thread plug technique of Zea Longa[20] with some modifications. Briefly, rats were anesthetized by intraperitoneal injection of 3.5% chloral hydrate (1 ml/100 g) and placed in the supine position on a platform. The skin was cut along the median cervical line. The left common carotid artery (CCA), external carotid artery (ECA) and internal carotid artery (ICA) were separated. The CCA and ECA were ligated in the proximal regions. The ICA was temporarily blocked with a slipknot tied with thin suture. A "V" incision was made 4 mm away from the CCA bifurcation. A fish wire (d = 0.265 mm), marked with lines at a length of 20–22 mm, was slowly inserted into the ICA through the CCA "V" incision and pushed with ophthalmic forceps until an insertion depth from the bifurcation of approximately 18 mm. Then, the outer end of the wire was fixed, and the skin incision was closed by ligature. In the sham operation group, the CCA, ECA and ICA were isolated, but no plug was inserted, and the rest of the procedure was as described above. Neurological deficits were assessed according to the Zea Longa scale.[20] In this study, rats with scores of more than 2 were included in the experiment, unless the rat died.

2, 3, 5-triphenyltetrazolium chloride (TTC) staining

Briefly, brain tissues were rapidly removed after sacrifice and frozen at −20 °C for 5 min and sliced into 5–6 uniform coronal slices. The slices were then immersed in 2% TTC (Sigma) at 37 °C in a water bath for 30 min away from light and fixed with 4% phosphate-buffered formalin before imaging. Then, the slices were arranged and photographed by a camera. Image J software was used to analyze the infarct volume.

Tissue processing and immunofluorescence staining

Anesthetized rats were transcardially perfused with 0.9% saline, followed by ice-cold 4% paraformaldehyde. The brains were removed and postfixed by immersion in 4% paraformaldehyde overnight at 4 °C. After postfixation, these brains were placed in 30% sucrose in PBS at 4 °C until they sank to the bottom. Serial 10 μm thick coronal sections through the infarct region were cut sequentially at −20 °C with a cryostat (Leica Instruments, CM1860, Germany). The sections of each group were incubated in a blocking solution at 37 °C for 30 min. Subsequently, each coronal section was treated with the primary antibodies. To identify the MCT1 distribution patterns in the sham and ischemic brain sections, chicken anti-MCT1 (1:100 in PBS, #AB1286-I, Millipore, USA) and mouse anti-GFAP (glial fibrillary acidic protein; 1:200 in PBS, #3670, CST, USA) primary antibodies

were applied. Then, the sections were washed three times with PBS for 10 min and incubated with appropriate secondary antibodies (1:200, FITC-conjugated donkey anti-chicken IgG, #D110201, Sangon Biotech; Cy3-conjugated goat anti-mouse IgG, #A0521, Beyotime, China) for 1 h at 37 °C. To facilitate proper photographic orientation, sections were counterstained with the nuclear dye 4′6-diamidino-2-phenylindole (DAPI, 1:100). The samples were analyzed under a confocal microscope (LSM510 Meta, Zeiss, Oberkochen, Germany) after mounting.

Western blotting analysis

Brain tissue (approximately 50 mg) from the ischemic region or ischemic penumbra were lysed with 400—500 μl of RIPA buffer (Beyotime, China) by sonication. After centrifugation, total protein amounts were determined in the supernatant. Equal amounts of protein were separated by 10% sodium dodecyl sulfate—polyacrylamide gel electrophoresis (SDS—PAGE) and transferred onto PVDF membranes. After overnight incubation with anti-MCT1 primary antibody (1:1000, Millipore AB1286-I, USA), the samples were washed with PBS for 30 min, followed by the addition of HRP-labeled anti-chicken secondary antibodies (1:200, Sangon Biotech, China) for 1 h at 37 °C. Anti-β-actin primary (1:1000, Beyotime, China) and HRP-labeled anti-mouse secondary (1:200, Origene, China) antibodies were used to assess β-actin as a loading control. The ECL kit (Bio-Rad, USA) was used to detect protein signals. Quantity one software was used to analyze the strip gray value of the exposure images.

Prediction and validation of miRNAs targeting MCT1

It was known that MCT1 was encoded by the *Slc16a1* gene through bioinformatics software. The bioinformatics software programs TargetScanHuman and microRNA.org were used to predict miRNAs targeting the rat *Slc16a1* gene. Rno-miR-124 was retrieved by both programs. TargetScanHuman demonstrated that the rno-miR-124-3p sequence complemented the 3′-UTR of *Slc16a1*. Therefore, the rno-miR-124-3p sequence was entered into the miRDB database and the Diana tool to predict target genes. It was therefore inferred that rno-miR-124-3p would likely target the *Slc16a1* gene in rats. Then, rno-miR-124-3p was validated by a double luciferase labeling test. Firstly, primers were designed according to the 3′-UTR of the *Slc16a1* (*Rattus*) gene. Then, the 3′-UTR sequence of *Slc16a1* was amplified by PCR using C6 genomic DNA as the template and cloned into the pmir-rb-report™ luciferase reporter vector. The fluorescence carrier was *hrluc*, with *hluc* as a reference for fluorescence correction. To assess whether rno-miR-124-3p directly regulates *Slc16a1* by targeting its 3′-UTR, wild-type and mutant *Slc16a1* 3′-UTR reporter genes were constructed by Guangzhou Ribo Bio Co., Ltd. After 293T cells were cotransduced with the rno-miR-124-3p mimic and the respective reporters, a Renilla luciferase vector (pRL-TK) was used to normalize the transfection efficiency. Cells were harvested 24 h after transfection and assayed with Luciferase Assay System (Promega, Madison, WI) according to the manufacturer's instructions. All assays were performed in triplicate and independently repeated more than three times.

Injection of rno-miR-124-3p agomir into the lateral ventricle of rats

Rats were randomly divided into 3 groups, the pMCAO group, the rno-miR-124-3p agomir + pMCAO group and the rno-miR-124-3p agomir control + pMCAO group, and two time points, 6 h and 24 h, were examined in each group. Briefly, rats were anesthetized by intraperitoneal injection of 3.5% ml/100 g chloral hydrate. Once anesthetized, rats were placed in the prone position with heads fixed in a stereotaxic instrument. Iodine was used to sterilize the scalp, followed by alcohol. The scalp was cut along the midline and 3% H_2O_2 was used to degrease and expose the skull, according to the book "The Rat Brain in Stereotaxic Coordinates" by Paxinos and Watson. The previous fontanel was set at 0. The entry point was 0.8—1.0 mm posterior and 1.2—1.5 mm from the midline, and the needle was inserted to 4—4.5 mm under the dura. According to these coordinates, a small hole was manually drilled in the corresponding part of the skull with a 50 ml syringe needle. Then, a 5 μl microsyringe was fixed on the stereoscopic positioner and fed vertically into the needle, and 5 μl agomir or agomir control (synthesized by Guangzhou Ribo Bio Co., Ltd) was injected into the left ventricle at a concentration of 100 pmol/L, with an injection rate of 1 μl/min. The syringe was left in place for 10 min to allow the solution to diffuse locally before removal. Then, the hole was sealed with medical bone wax, and the skin was sutured after local disinfection. Rats were resuscitated on the thermostatic operating table, and the pMCAO surgery was conducted a week later. The rats in the pMCAO groups were not injected. One week later, the rats were given pMCAO surgery and the Zea Longa scoring method was used to determine the success of model establishment. Upon successful modeling, after 6 h or 24 h of pMCAO, the rats were killed and their brains were removed for mRNA, protein detection and injury evaluation. The tissue was separated into two parts, including the left cerebral cortex containing the ischemic region and the penumbra.

RNA isolation, reverse transcription and quantitative real-time PCR (qRT-PCR)

Rats were anaesthetized and perfused with saline until the liver and kidney turned white. Then, the brain tissue was extracted gently. The left cerebral cortex was separated into two parts, including the ischemic region and the penumbra, according to the position of the middle cerebral artery. Total RNA (and miRNA) in brain samples was extracted with RNAiso Plus (Takara, China) according to the manufacturer's protocol. Reverse transcription of mRNA was performed using a reverse transcription kit (Takara, #RR047A), and reverse transcription of miRNA was performed using a Mir™-X miRNA First-Strand Synthesis Kit (Clontech, #638313). Then, the reverse transcription products were diluted 5-fold and stored at −80 °C. QRT-PCR was performed to quantify MCT1 mRNA and rno-miR-124-3p levels according to the manufacturer's instructions for

SYBR® premix Ex Taq™ II (Takara, Tli RNaseH Plus, #RR820A). The levels of MCT1 mRNA and rno-miR-124-3p before/after agomir lateral ventricle administration were assessed on a CFX96™ real-time PCR detection system. The primers (Takara, China) used were Rattus MCT1 (sense 5′-TGCTGGCACCTTTGTCTACGA-3′ and anti-sense 5′-CCAGGAGACAGGACAACATTC-3′), and rno-miR-124-3p: TAAGGCACGCGGTGAATGCC. Both reverse transcription and qRT-PCR were performed in 3 separate triplicate experiments. The relative expression levels of rno-miR-124-3p and MCT1 mRNA were normalized to those of the internal control U6 and β-actin using a $2^{-\Delta\Delta Ct}$ cycle threshold method.

Statistical analysis

All data were analyzed with SPSS 19.0 software (Chicago, IL, USA). All data are presented as the means ± SD and were tested for normality. Differences between individual groups were initially compared using one-way ANOVA. Then, data were analyzed with the LSD multiple-comparison post hoc test. Student's *t*-test was used to analyze the difference between two groups. All of the reported *p*-values were two-sided and $p < 0.05$ was considered statistically significant. The figures were generated with the GraphPad Prism 5.0 software.

Results

MCT1 expression was increased after pMCAO

MCT1 was expressed on microvessels and ependymocytes (Fig. 1A and B) in both sham and experimental rat brains. Compared with the sham group, MCT1 expression was increased both in cortext and ependymocytes, up to 6 h after ischemia. The results of the double immunofluorescence of MCT1 and GFAP, a marker of astrocytes, showed that MCT1 was only coexpressed at the foot of the astrocytes, close to the microvessels.

Slc16a1 is a target gene of rno-miR-124-3p

TargetScanHuman showed that the 3′-UTR of *Slc16a1* contained the binding site of rno-miR-124-3p. Double luciferase reporter gene experiments validated that 293T cells transfected with rno-miR-124-3p mimic exhibited luciferase activity reduced by nearly 30% when the wild-type *Slc16a1* carrier was used compared with the *Slc16a1*-WT + NC group. As expected, the luciferase activity of the mutant *Slc16a1* carrier showed no significant change when co-expressed with rno-miR-124-3p (Fig. 2). These results demonstrated that *Slc16a1* was targeted by rno-miR-124-3p.

Expression levels of MCT1 protein and rno-miR-124-3p after pMCAO

Western blotting analysis showed that the MCT1 protein level gradually increased with the extension of ischemic time to 24 h after pMCAO both in the ischemic region and penumbra; in particular, it appeared to sharply increase at 1 h of pMCAO (Fig. 3 A1, A2, B1, B2). QRT-PCR analysis showed that the expression of rno-miR-124-3p after pMCAO was in contrast to the expression of MCT1 in the ischemic region, while declined after 3 h, 6 h and 12 h of pMCAO in ischemic penumbra (Fig. 3 A3, B3).

Administration of rno-miR-124-3p agomir changed MCT1 expression

In the ischemic region, the MCT1 levels in the agomir group increased after 6 h of pMCAO, while slightly decreased after 24 h of pMCAO (Fig. 4 A1, A3). The tendency of MCT1 protein expression changes in the ischemic penumbra was in accordance with that in the ischemic region both after 6 h and 24 h of pMCAO (Fig. 4 A2, A4). The levels of MCT1 mRNA in agomir group were increased after 6 h of pMCAO but decreased after 24 h of pMCAO both in the ischemic region and ischemic penumbra, while the rno-miR-124-3p levels were upregulated both after 6 h and 24 h in the ischemic region and ischemic penumbra, although there were no significant changes after 6 h of pMCAO in the ischemic region (Fig. 4 B).

Administration of rno-miR-124-3p reduced brain infarction

TTC reacts with a functioning mitochondrial electron transport chain to generate a red color in normal brain tissue that contrasts with the white color of the infarction. The brain tissue slices of the sham group appeared pink upon TTC staining. After 6 h of ischemia, TTC staining defects were clearly identified in the cortex and dorsolateral striatum. The white region was slightly reduced in the rno-miR-124-3p agomir + pMCAO-6 h group. After 24 h of ischemia, the white regions extended to most of the middle cerebral artery supplied territory and went more deeply. Compared with the pMCAO-24 h group, the infarct regions were significantly decreased in the rno-miR-124-3p agomir + pMCAO-24 h group (Fig. 5).

Discussion

Studies have reported that MCT1 is predominantly found on endothelial cells forming cerebral blood vessels and on astrocytes.[11,21–23] In this study, similarly, MCT1 was mainly expressed on the microvessels, the foot of astrocytes facing microvessels and ependymocytes, which were all close to the blood or cerebrospinal fluid (Fig. 1). During the acute phase of cerebral ischemia, persistent ischemia and hypoxia resulted in the accumulation of lactic acid, and the expression level of MCT1 increased over that duration of time. Some researchers have revealed that MCT1 mRNA expression is significantly increased after permanent stroke.[24] In addition, decreased activity of MCT1 in the cerebral microvasculature may be a critical determinant of acid-related cell damage during stroke, as evidenced by the fact that lactic acid is not cleared from the brain during cerebral ischemia.[9] Similarly, overexpression of MCT1 mRNA in the brain is correlated with reduced cell damage following experimental transient focal cerebral ischemia in

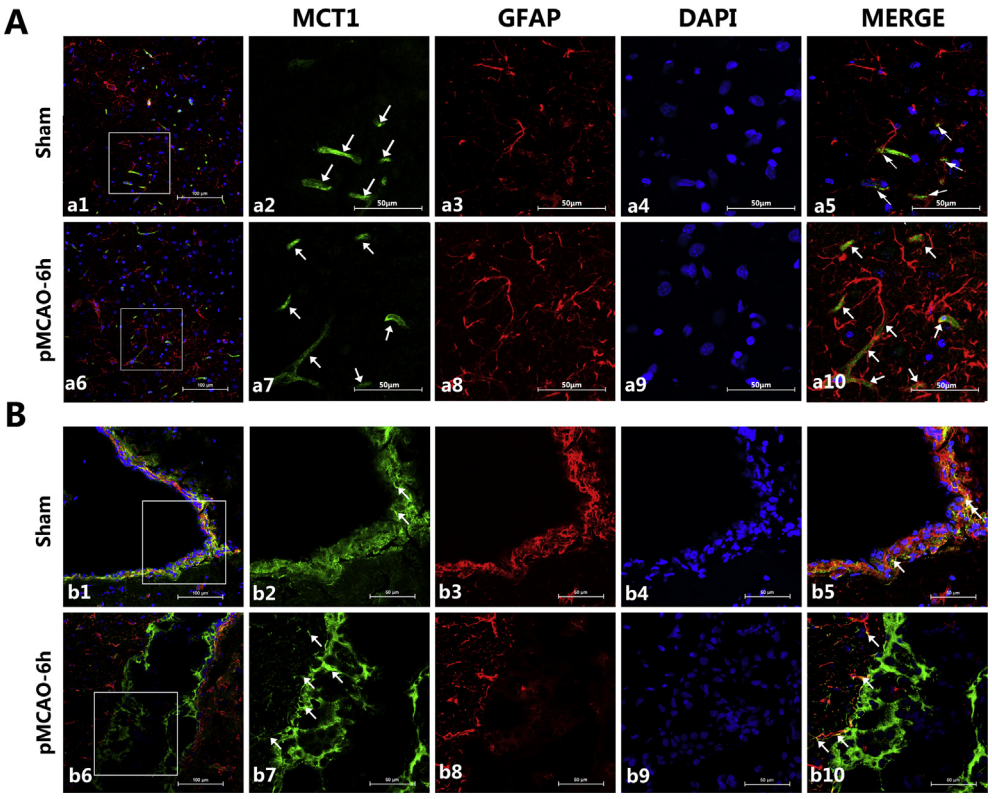

Figure 1 Representative expression of MCT1 at corresponding times after pMCAO. (A) Confocal images showing the expression of MCT1 and GFAP in cerebral cortex. MCT1 (green), GFAP (red), and nuclei (blue). For the sham group, a1 represents the merge of the three colors at 200 times magnification. Magnifying the white square to 600 times is represented in a2, a3 and a4. Merging a2, a3 and a4 resulted in a5. The effects of pMCAO at 6 h is represented in a similar way to that of sham group. It can be seen that MCT1 was expressed in microvessels (shown with white arrows in a2 and a7) and the astrocytic foot (shown with white arrows in a5 and a10); moreover, it can be seen in a5 and a10 that many protrusions of astrocytes were located tightly around capillaries, especially in the pMCAO-6h group. (B) Confocal images showing the expression of MCT1 and GFAP in ependymocytes. The presentation is the same as A, however, the last four pictures of each group were magnified 400 times. MCT1 was highly expressed in ependymocytes, especially in the pMCAO-6h group, and the coexpression of MCT1 and GFAP was still visible.

rodents.[25] In the present study, the changes in the expression levels of MCT1 in brain tissues detected by Western blotting were increased after pMCAO (Fig. 3). For MCT1 regulation, researchers have suggested that the intracellular pH of cerebrovascular endothelial cells could control MCT1 function.[26] Meanwhile, it was found that cAMP signaling reduces the functionality of MCT1 in cerebrovascular endothelial cells by facilitating its entry into a highly dynamic vesicular trafficking pathway that appears to lead to the transporter's trafficking to autophagosomes and lysosomes.[27] In addition, miR-124 is frequently downregulated in medulloblastoma of humans and negatively regulates *Slc16al*.[28] However, the regulation of MCT1 by miRNAs in cerebral ischemia has not been previously reported.

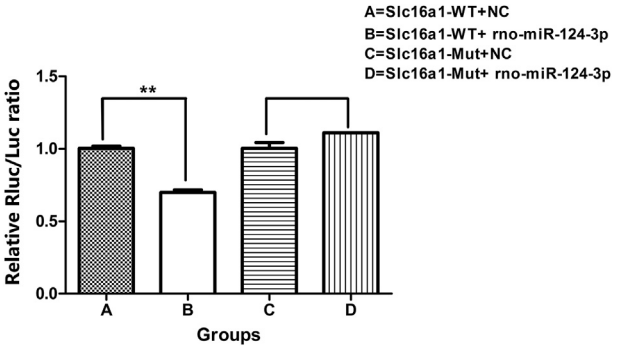

Figure 2 Results of the double luciferase reporter assay. A: *Slc16a1*-WT + NC; B: *Slc16a1*-WT + rno-rno-miR-124-3p; C: *Slc16a1*-Mut + NC; D: *Slc16a1*-Mut + rno-miR-124-3p. $^{**}p < 0.01$ vs *Slc16a1*-WT + NC group. (NC: abbreviation of normal control; Mut: abbreviation of mutant; WT: abbreviation of wild type.)

MicroRNAs are a family of important posttranscriptional regulators of gene expression that bind to mRNA targets to induce their degradation or repress translation. It had been demonstrated that miRNAs are involved in the pathophysiology of cerebrovascular disease.[2] Furthermore, almost all ischemic conditions lead to altered circulating miRNA levels.[29] Therefore, miRNAs may represent potential diagnostic and therapeutic tools in clinical practice. Considering the important role of MCT1 in mediating the transportation of lactic acid during cerebral ischemia, we asked whether miRNAs are involved in the regulation of MCT1 in cerebral ischemia. Thus, in this study, the miRNAs likely targeting MCT1 were detected by bioinformatics and

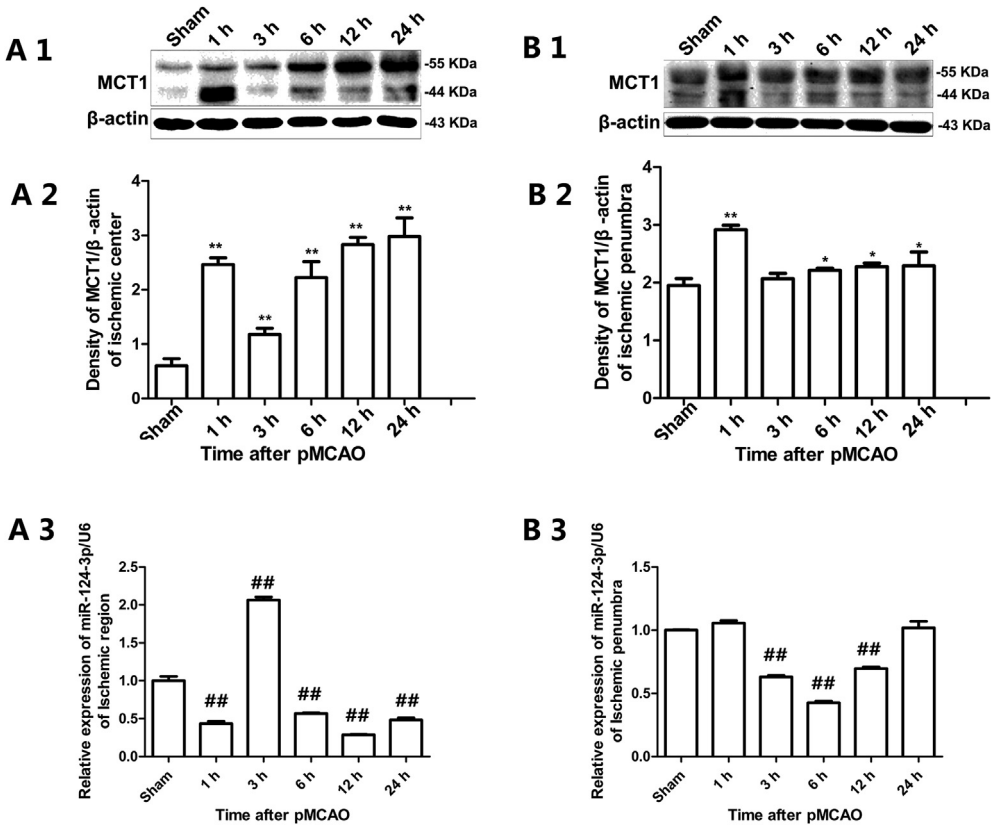

Figure 3 Expression of MCT1 protein and **rno-miR-124-3p** after pMCAO. A1, A2, B1 and B2 were results of Western blotting analysis. A3 and B3 were results of qRT-PCR analysis. Data are represented as the means ± SD. *#Significant difference between the sham and pMCAO groups (A1, A2 and A3: ischemic region; B1, B2 and B3: ischemic penumbra. *$p < 0.05$, vs. sham group; **$p < 0.01$ vs. sham group; ##$p < 0.01$, vs. sham group. n = 3 in each group).

validated by a double luciferase reporter assay. The results suggested that *Slc16a1* is a genuine target of rno-miR-124-3p (Fig. 2).

MiR-124, almost exclusively expressed in the central nervous system and neuronal cells, shows 100 times higher expression there than in other organs. Studies have demonstrated that miR-124 could target a number of mRNAs, such as VSNL1,[30] Ku70,[31] Usp14,[32] Bcl-2 and Bcl-xl,[33] and iASPP[34] in stroke. It was reported that miR-124 acts as a biomolecule in neuroprotective therapy of cerebral ischemia.[35] The authors clearly pointed out that miR-124 has a strong protective effect on the CNS tissue and stated that such an impact was strongly visible within the first week after MCAO. Researchers demonstrated that a sufficient miR-124 concentration is crucial for its effectiveness.[35,36] Hence, miR-124 may have multiple and complex roles in cerebral ischemia. However, whether rno-miR-124-3p could play a protective role by targeting MCT1 during cerebral ischemia in vivo remained unclear. Therefore, we synthesized rno-miR-124-3p agomir and conducted experiments in rats for further confirmation. As the efficacy of agomir could maintain more than 6 weeks (seen in the product manual for details), we performed pMCAO surgery one week after rno-miR-124-3p agomir lateral ventricle administration. The alteration in levels of rno-miR-124-3p and MCT1 mRNA together with its protein expression were examined, and the infarction area was also detected by TTC staining after pMCAO. To our surprise, after rno-miR-124-3p agomir was injected, the levels of MCT1 mRNA and its protein expression were increased in the ischemic region and penumbra. Meanwhile, the expression level of rno-miR-124-3p was slightly increased after 6 h of pMCAO. The levels of MCT1 mRNA and its protein expression were downregulated after 24 h of pMCAO, while the rno-miR-124-3p level was upregulated after 24 h of pMCAO (Fig. 4). According to the principle of molecular biology, the sequences of rno-miR-124-3p should combine with the 3′-UTR sequences of MCT1, resulting in decreased MCT1 expression. It seems that an increased expression of MCT1 in the rno-miR-124-3p agomir group after 6 h ischemia is contrary to the principle. Why did is happen? In our opinion, at the early ischemic stage in the brain, a large volume of lactic acid accumulated in the extracellular space, and then, the accumulated lactic acid might activate other signal molecules associated with MCT1 expression, which upregulated the expression level of MCT1, accelerating the transportation of lactic acid. Therefore, at 6 h after pMCAO, the level of MCT1 expression was upregulated in the rno-miR-124-3p agomir group. The results of TTC staining showed that the infarction area was reduced after both 6 h and 24 h of pMCAO in the agomir group (Fig. 5). As mentioned above, miR-124 acts as a biomolecule in neuroprotective therapy of cerebral ischemia and has a strong protective effect on the CNS

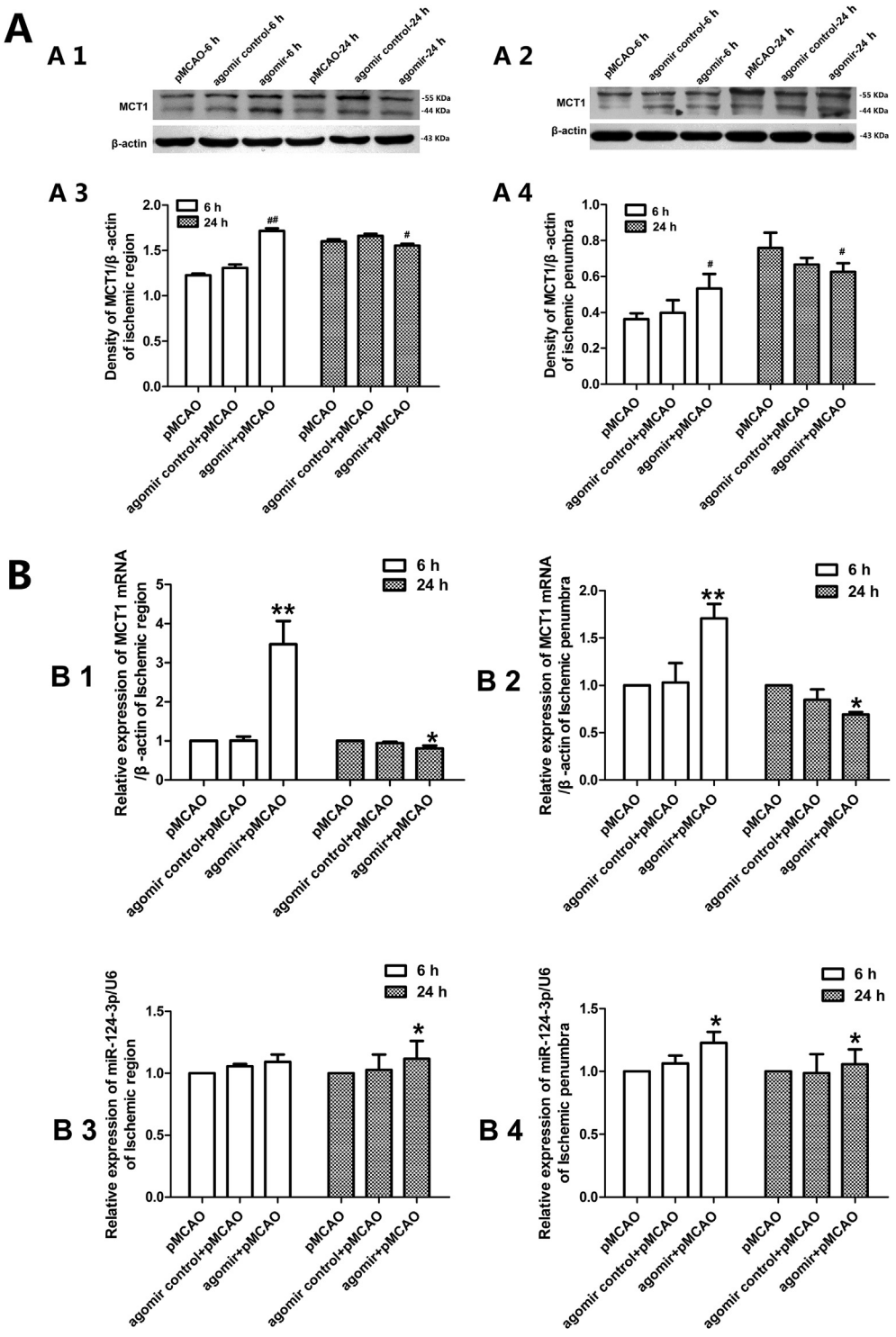

Figure 4 Expression levels of MCT1 protein, MCT1 mRNA and rno-miR-124-3p detected after rno-miR-124-3p agomir lateral ventricle administration. (A) Western blotting detection of MCT1 protein expression at corresponding times after pMCAO (A1 and A3: ischemic region; A2 and A4: ischemic penumbra; n = 3, $^{\#}p < 0.05$, vs. pMCAO group; $^{\#\#}p < 0.01$ vs. pMCAO group). (B) qRT-PCR detection of MCT1 mRNA and rno-miR-124-3p after rno-miR-124-3p agomir lateral ventricle administration (B1 and B3: ischemic region; B2 and B4: ischemic penumbra; B1 and B2: Levels of MCT1 mRNA; B3 and B4: Levels of rno-miR-124-3p; n = 3, $^{*}p < 0.05$, vs. pMCAO group; $^{**}p < 0.01$ vs. pMCAO group).

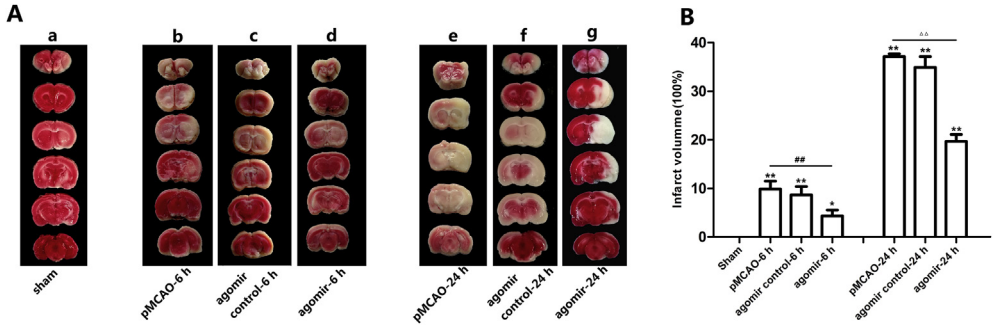

Figure 5 Representative TTC-stained brain slices showing tissue infarction, which is shown as a white region. No appreciable TTC staining defects were observed in the sham rat brains (a). After 6 h of ischemia, TTC staining defects were clearly identified in the cortex and dorsolateral striatum (b, c, d), and the white region was slightly reduced in the rno-miR-124-3p agomir + pMCAO-6 h group (d). After 24 h of ischemia, the white regions extended to most of the middle cerebral artery supplied territory and went more deeply (e, f, g). Compared to the pMCAO-6 h group (e), the infarct regions were significantly decreased in the pMCAO-6 h + rno-miR-124-3p agomir group (g). Similarly, the infarct regions were significantly decreased in the pMCAO-24 h + rno-miR-124-3p agomir group (g), comparing with the pMCAO-24 h group (e). (a: sham group; b: pMCAO-6 h group; c: rno-miR-124-3p agomir control + pMCAO-6 h group; d: rno-miR-124-3p agomir + pMCAO-6 h group; e: pMCAO-24 h group; f: rno-miR-124-3p agomir control + pMCAO-24 h group; g: rno-miR-124-3p agomir + pMCAO-24 h group. $^{*}p < 0.05$, $^{**}p < 0.01$, vs. sham group; $^{\#\#}p < 0.01$ vs. pMCAO-6 h group; $^{\triangle\triangle}p < 0.01$ vs. pMCAO-24 h group. n = 3 in each group).

tissue. Thus, the role of rno-miR-124-3p in regulating MCT1 expression should be taken into account when using miR-124 as a drug target for the early treatment of cerebral ischemia.

In summary, we demonstrated for the first time that MCT1 was a target of rno-miR-124-3p. Rno-miR-124-3p plays a protective role by regulating the expression of MCT1 under cerebral ischemia. In the present experiment, we found that the expression level of MCT1 after 6 h of pMCAO in the rno-miR-124-3p agomir group was higher than that in the pMCAO group, which implied that there might be other molecular mechanisms of MCT1 expression regulation under ischemic conditions in addition to miRNA mechanisms. Thus, future studies are necessary to illuminate the more regulatory mechanisms of MCT1 in early-stage cerebral ischemia.

Conflicts of interest

The authors have no relevant conflicts of interest to disclose.

References

1. Roger VL, Go AS, Lloyd-Jones DM, et al. Heart disease and stroke statistics—2011 update: a report from the American Heart Association. *Circulation*. 2011;123(4):e18—e209.
2. Volny O, Kasickova L, Coufalova D, Cimflova P, Novak J. microRNAs in cerebrovascular disease. *Adv Exp Med Biol*. 2015; 888:155—195.
3. Pellerin L, Magistretti PJ. Glutamate uptake into astrocytes stimulates aerobic glycolysis:A mechanism coupling neuronal activity to glucose utilization. *Proc. Natl. Acad. Sci. U.S.A.* 1994;91(22):10625—10629.
4. Jalloh I, Helmy A, Shannon RJ, et al. Lactate uptake by the injured human brain: evidence from an arteriovenous gradient and cerebral microdialysis study. *J Neurotrauma*. 2013;30(24): 2031—2037.
5. Morrison BM, Tsingalia A, Vidensky S, et al. Deficiency in monocarboxylate transporter 1 (MCT1) in mice delays regeneration of peripheral nerves following sciatic nerve crush. *Exp Neurol*. 2015;263:325—338.
6. Bouzat P, Sala N, Suys T, et al. Cerebral metabolic effects of exogenous lactate supplementation on the injured human brain. *Intensive Care Med*. 2014;40(3):412—421.
7. Rice AC, Zsoldos R, Chen T, et al. Lactate administration attenuates cognitive deficits following traumatic brain injury. *Brain Res*. 2002;928:156—159.
8. Holloway R, Zhou Z, Harvey HB, et al. Effect of lactate therapy upon cognitive deficits after traumatic brain injury in the rat. *Acta Neurochir*. 2007;149(9):919—927.
9. Smith JP, Drewes LR. Modulation of monocarboxylic acid transporter-1 kinetic function by the cAMP signaling pathway in rat brain endothelial cells. *J Biol Chem*. 2006;281(4): 2053—2060.
10. Martinov V, Rizvi SM, Weiseth SA, Sagave J, Bergersen LH, Valen G. Increased expression of monocarboxylate transporter 1 after acute ischemia of isolated, perfused mouse hearts. *Life Sci*. 2009;85(9-10):379—385.
11. Moreira TJ, Pierre K, Maekawa F, et al. Enhanced cerebral expression of MCT1 and MCT2 in a rat ischemia model occurs in activated microglial cells. *J Cerebr Blood Flow Metabol—Off J Int Soci Cerebr Blood Flow Metabol*. 2009;29(7):1273—1283.
12. Halestrap AP, Meredith D. The *SLC16* gene family-from monocarboxylate transporters (MCTs) to aromatic amino acid transporters and beyond. *Pflueg Arch Eur J Physiol*. 2004; 447(5):619—628.
13. Perez-Escuredo J, Van Hee VF, Sboarina M, et al. Monocarboxylate transporters in the brain and in cancer. *Biochim Biophys Acta*. 2016;1863(10):2481—2497.
14. Bartel DP. MicroRNAs:Genomics, review biogenesis, mechanism, and function. *Cell*. 2004;116(2):281—297.
15. Sun E, Shi Y. MicroRNAs: small molecules with big roles in neurodevelopment and diseases. *Exp Neurol*. 2015;268:46—53.
16. Ouyang Y-B, Creed M, Stary M, Guo-Yuan Yang M, Rona Giffard M. microRNAs: innovative targets for cerebral ischemia and stroke. *Curr Drug Targets*. 2013;14(1):90—101.
17. Wu P, Zuo X, Ji A. Stroke-induced microRNAs: the potential therapeutic role for stroke. *Exp Therapeut Med*. 2012;3(4): 571—576.

18. Bhalala OG, Srikanth M, Kessler JA. The emerging roles of microRNAs in CNS injuries. *Nat Rev Neurol*. 2013;9(6):328—339.
19. Vemuganti R. The MicroRNAs and stroke: No need to be coded to be counted. *Transl Stroke Res*. 2010;1(3):158—160.
20. Longa EZ, Weinstein PR, Carlson S, Cummins R. Reversible middle cerebral artery:occlusion without craniectomy in rat. *Stroke*. 1989;20:84—91.
21. Pierre K, Pellerin L, Debernardi R, Riederer B, Magistretti P. Cell-specific localization of monocarboxylate transporters, MCT1 and MCT2, in the adult mouse brain revealed by double immunohistochemical labeling and confocal microscopy. *Neuroscience*. 2000;100(3):617—627.
22. Hanu R, McKenna M, O'Neill A, Resneck W, Bloch R. Monocarboxylic acid transporters, MCT1 and MCT2, in cortical astrocytes in vitro and in vivo. *Am J Physiol Cell Physiol*. 2000; 278(5):C921—C930.
23. Gerhart DZ, Enerson BE, Zhdankina OY, Leino RL, Drewes LR. Expression of monocarboxylate transporter MCT1 by brain endothelium and glia in adult and suckling rats. *AJP (Am J Physiol)*. 1997;273(1 Pt 1):E207—E213.
24. Geng X, Sy CA, Kwiecien TD, et al. Reduced cerebral monocarboxylate transporters and lactate levels by ethanol and normobaric oxygen therapy in severe transient and permanent ischemic stroke. *Brain Res*. 2015;1603:65—75.
25. Pierre K, Pellerin L. Monocarboxylate transporters in the central nervous system: distribution, regulation and function. *J Neurochem*. 2005;94(1):1—14.
26. Uhernik AL, Tucker C, Smith JP. Control of MCT1 function in cerebrovascular endothelial cells by intracellular pH. *Brain Res*. 2011;1376:10—22.
27. Uhernik AL, Li L, LaVoy N, Velasquez JM, Smith JP. Regulation of monocarboxylic acid transporter-1 by cAMP dependent vesicular trafficking in brain microvascular endothelial cells. *PLoS One*. 2014;9(1), e85957.
28. Li KK, Pang JC, Ching AK, et al. miR-124 is frequently down-regulated in medulloblastoma and is a negative regulator of *Slc16a1*. *Hum Pathol*. 2009;40(9):1234—1243.
29. van Empel VP, De Windt LJ, da Costa Martins PA. Circulating miRNAs: reflecting or affecting cardiovascular disease? *Curr Hypertens Rep*. 2012;14(6):498—509.
30. Jeyaseelan K, Lim KY, Armugam A. MicroRNA expression in the blood and brain of rats subjected to transient focal ischemia by middle cerebral artery occlusion. *Stroke*. 2008;39(3):959—966.
31. Di Y, Lei Y, Yu F, Changfeng F, Song W, Xuming M. MicroRNAs expression and function in cerebral ischemia reperfusion injury. *J Mol Neurosci—MN*. 2014;53(2):242—250.
32. Doeppner TR, Doehring M, Bretschneider E, et al. MicroRNA-124 protects against focal cerebral ischemia via mechanisms involving Usp14-dependent REST degradation. *Acta Neuropathol*. 2013;126(2):251—265.
33. Sun Y, Gui H, Li Q, et al. MicroRNA-124 protects neurons against apoptosis in cerebral ischemic stroke. *CNS Neurosci Ther*. 2013;19(10):813—819.
34. Liu X, Li F, Zhao S, et al. MicroRNA-124-mediated regulation of inhibitory member of apoptosis-stimulating protein of p53 family in experimental stroke. *Stroke*. 2013;44(7):1973—1980.
35. Hamzei Taj S, Kho W, Riou A, Wiedermann D, Hoehn M. MiRNA-124 induces neuroprotection and functional improvement after focal cerebral ischemia. *Biomaterials*. 2016;91:151—165.
36. Willemen HL, Huo X-J, Mao-Ying Q-L, Zijlstra J, Heijnen CJ, Kavelaars A. MicroRNA-124 as a novel treatment for persistent hyperalgesia. *J Neuroinflammation*. 2012;9:143.